Progress In Electromagnetics Research M, Vol. 107, 91–103, 2022

Proximity Fed Triple Band David Fractal 2×1 Microstrip Patch Array Antenna with DGS

Jacob Abraham*

Abstract—This paper presents a triple band proximity fed 2×1 array antenna with defected ground plane. The proposed antenna configuration is composed of two radiating elements, and both radiating elements are made of a pattern similar to the first iteration level David fractal geometry. The proposed David fractal 2×1 array antenna is designed and simulated on an FR-4 substrate of thickness 1.6 mm and dielectric constant 4.3 by using the CST Microwave Studio simulation tool. In order to improve the radiation characteristics of the antenna, an H-shaped defect is etched in the ground plane. The antenna is fabricated and tested. The experimental data show good agreements with simulation results. The fabricated triple band fractal 2×1 array antenna resonates at 2.527 GHz, 3.329 GHz, and 3.742 GHz having bandwidths of 303 MHz, 99 MHz, and 102 MHz, respectively. The proposed fractal array antenna can be used in mobile applications such as Wi-Fi, WLAN, Bluetooth, and Wi-Max.

1. INTRODUCTION

In recent years, there have been a rapid and tremendous growth in the field of wireless communication due to the invention of portable handled communication device and also because of raising high speed internet penetration. This portable device requires antennas with smaller dimensions and multiband characteristics. This requirement has initiated research actives in various directions to develop smaller antennas. Microstrip antennas become popular among antenna designers since they offer many advantages like extremely low profile, light weight, simplicity, and are inexpensive to fabricate using modern day printed circuit board technology. They are also compatible with microwave and millimetre-wave integrated circuits. A simple microstrip patch antenna consists of a conducting patch and a ground plane, and between them is a dielectric medium called the substrate having a particular value of dielectric constant. The dimensions of a patch are smaller than that of substrate and ground. Microstrip patch antenna is a well suited device for wireless communication devices and can work at multiple frequencies [1, 2]. In the following paragraphs, designing issues related with microstrip patch antennas are analysed. Various feeding techniques used to excite patch antennas are mentioned in the second paragraph. Conventional microstrip antennas had some limitations, incuding single operating frequency as well as low impedance bandwidth. There are a number of techniques which have been reported for enhancing the above mentioned parameters and are presented in the third paragraphs. The defected ground structure and its significances in the field of patch antenna design are discussed in the fourth paragraph. In the fifth paragraph, the use of fractal geometries in the antenna design is explained, and in the last paragraph, works related to the proposed fractal 2×1 array antenna are discussed.

Different feeding techniques are used to excite the microstrip patch antenna and are generally classified into contacting and non-contacting types. In the first type, RF power is fed directly to the radiating elements. Most commonly used contacting feed methods are microstrip line feed [3] and

Received 13 December 2021, Accepted 6 January 2022, Scheduled 11 January 2022
* Corresponding author: Jacob Abraham (tjacobabra@gmail.com).
The author is with the Department of Electronics, B P C College, Piravom, Kerala, India.

coaxial feed [4]. Proximity feeding [5] and aperture feeding [6] are common types of non-contact feeding techniques, where power is transferred to the radiating elements from feed line using electromagnetic coupling. Several research articles are available where these feeding techniques have been studied and compared [7–9]. Proximity feeding offers several merits over other methods such as large bandwidth and low spurious radiation. A novel proximity-coupled fed microstrip circular patch antenna resonating at a frequency of 3.5 GHz is proposed for 5G applications [10]. Many researchers have also focused their work on developing multiband antennas where radiating element is excited using proximity feeding technique [11, 12].

With the rapid development in the field of wireless communication, a modern wireless communication network offers multiple services which supports various standards and mobile cellular system like: GSM, PCS, UMTS, WLAN, Wi-Fi, Wi-MAX, LTE, Bluetooth, etc., hence the need of multiband antenna arises. Multiband antennas are developed to operate in multiple frequency bands. Multiband antennas use a design in which one part of the antenna is active for one band, while another part is active for a different band. A lot of techniques have been reported in literature to improve the above listed antenna parameters. Multiband operation was achieved by employing various techniques including stacking [13], defected ground structure [14], frequency selective surface FSS [15], Electromagnetic Band Gap (EBG) [16], Photonic Band Gap (PBG) [17], and by using Metamaterial [18]. Several other well established techniques have also been employed to convert a normal single band microstrip patch antenna into a multiband antenna such as cutting slots in the radiating patches [19], using dual fed technique [20], using parasitic patches with same dimensions as that of radiating patches [21], and a pair of double split ring resonators (DSRRs) on either side of the feed [22]. A common limitation for this type of antenna is narrow bandwidth. The typical impedance bandwidth of a microstrip antenna is between 1 and 2%. Many kinds of bandwidth enhancement techniques, such as increasing the patch-ground plane separation by using a thicker substrate [23], shorted patch [24], loading with parasitical patches [25], slot loading techniques [26], and slotted ground plane [27], have been proposed and applied to microstrip patch antennas.

Defected ground structure [DGS] enhances the performance of the microstrip patch antenna by intentionally modifying the ground plane metal of the patch antenna structure. DGS is realized by etching off a simple shape in the ground plane which is known as defect. The defects etched on the ground plane will disturb the shielded current distribution which results in controlled excitation and propagation of the electromagnetic waves through the substrate layer. The patch antenna with defected ground structure has a large electric length compared to a conventional patch antenna for the same physical length. The term DGS was first reported to describe a single unit of dumbbell shaped defect in the ground plane [28]. Studies are done to analyse the effect of various shapes of defects etched in the ground plane [29, 30]. Studies have also been reported regarding achieving multiband characteristics by using a defected ground structure [31]. Several research articles have reported that better return loss performances are achieved due to DGS [32, 33].

In recent years, fractal geometries have been widely used in patch antenna designs to reduce dimensions of the radiating elements and also to achieve multiband characteristics. Fractal geometries are composed of multiple iterations of a single elementary shape and can be continued infinite times thus forming a shape with in a finite boundary but of infinite length or area. Various fractal geometries have been utilized to develop multiband and miniaturized microstrip fractal antennas. In recent years, many intensive research works have been done using fractal geometries to develop useful radiating elements, such as Log Periodic Fractal Koch [34], Bow-Shaped Fractal Helix [35], Sierpinski gasket [36], plus shape [37], Durer pentagon fractal geometry [38], and Square Shaped Fractal [39]. Nowadays, microstrip patch antennas have been developed with pentagon and hexagon shaped radiating patches rather than the conventional square and rectangular shapes [40, 41].

The main aim of this paper is to present a new patch array antenna configuration that utilizes first iteration level David fractal geometry shape as radiating elements. David fractal [42] concept was effectively embedded in a hexagon shaped radiating patch antenna to achieve multiband characteristics and size reduction [43]. The reported dual band antenna configuration yields bandwidths of 3.05% and 0.91%, respectively, at lower and upper bands. In this proposed work, both radiating elements are etched on the top side of the upper substrate. An H-shaped defect is etched in the ground plane for improving antennas operating parameters and the return loss characteristics. The proposed 2×1

David fractal array antenna with DGS is excited using proximity fed coupling technique. In order to obtain optimized antenna parameters, simulation studies are carried out using CST Microwave Studio. Prototype of the proposed antenna was fabricated and tested in order to validate the simulated studies. The proposed antenna shows triple band characteristics with enhanced operating parameters compared to the reference antenna described in [43]. The operating frequencies of the antenna make it a suitable device in many portable wireless communication devices.

2. EVOLUTION OF THE ANTENNA GEOMETRY

This section discusses various evolution stages involved in the development of proximity fed David fractal 2×1 microstrip patch array antenna with DGS. The design process begins with a single band hexagon-shaped microstrip patch antenna as shown in Figure 1(a). In order to modify it to behave as a dual band antenna, first iteration level David fractal geometry has been embedded into the basic hexagon shape, and modified antenna geometry is as shown in Figure 1(b). In order to achieve triple band operation array concept was utilized as shown in Figure 1(c), by placing similar radiating elements with spacing in between. To further enhance return loss characteristics at higher band and for effective coupling of RF power from feed line to radiating patches, defects are etched in the ground plane. In this case, an H-shaped defect is etched in the ground plane to enhance antenna operating parameters by utilizing properties exhibited by defected ground plane.

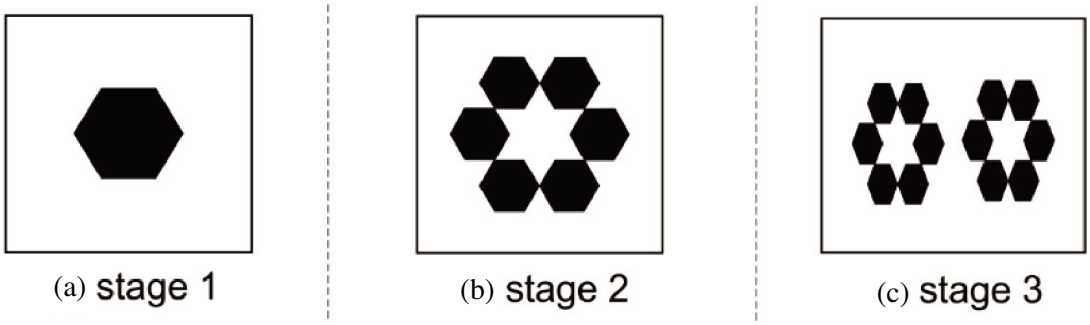

Figure 1. Evolution stages of the proposed antenna.

2.1. Antenna Design Procedure

The equations for the hexagonal microstrip patch antenna can be obtained from the resonant frequency equations of the circular microstrip patch antenna discussed in [43] by equating the respective areas as shown in Figure 2. The fundamental resonance frequency of a circular patch antenna is given by

$$f_r = \frac{X_{mn}C}{2\pi a_e\sqrt{\varepsilon_r}}$$

where

f_r = *resonant frequency of the patch*
X_{mn} = *1.8411 for the dominant mode* TM_{11}
C = *velocity of the light in free space*
ε_r = *relative permittivity of the substrate*
a_e = *effective radius of the circular patch and given by*
$a_e = a\{1 - 2h/\pi a\varepsilon, (\mathrm{In}\pi a/2h + 1.7726)\}^{0.5}$

In the above equation, 'a' is the actual radius of the circular patch antenna, and h is the height of the substrate. The above equations can be applied to design a hexagonal microstrip patch antenna by relating the areas of the circular and hexagonal patches as shown in equation given below.

$$\prod a_e^2 = \frac{3\sqrt{3}s^2}{2}$$

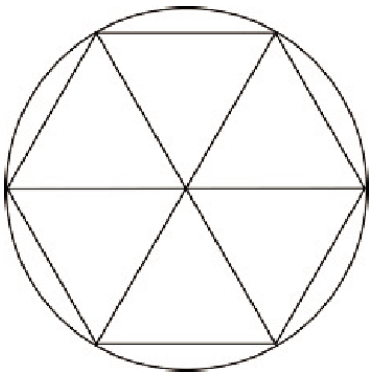

Figure 2. Formation of a hexagonal shape from a circle.

where 's' is the side length of the hexagonal patch.

The David fractal pattern is formed from the basic hexagon-shaped patch or initiator as shown in Figure 1(a), by dividing it into six smaller hexagons; six isosceles triangles and a David star at the center, then the triangles and star are removed. The length of the base of the isosceles triangle is found using $L_b = L \times 0.382^k$, where $k = 1, 2, 3, ...$ depending on the level of iteration. For the first level of iteration, the value of k is one, and for the second level of iteration the value of k is two. L is the length of side of hexagon where isosceles triangle is removed. It results in the formation of the first level of iteration as shown in Figure 1(b).

2.2. Antenna Configuration

Figure 3 presents the geometry of the proposed proximity fed David fractal 2×1 microstrip patch array antenna with DGS. The David fractal 2×1 array antenna has been designed on an FR-4 substrate with dielectric constant of 4.3, loss tangent of 0.001, and height of 1.6 mm. FR-4 is a grade designation assigned to glass reinforced epoxy laminate sheets rods and printed circuit boards. FR-4 is a composite material composed of woven fiberglass cloth with an epoxy resin binder that is flame resistant. It is a popular and versatile high pressure thermoset plastic laminate grade with good strength to weight ratios. With near zero water absorption, it is most commonly used as an electrical insulator possessing considerable mechanical strength. These attributes along with good fabrication characteristics helped in selecting this substrate for designing the proposed antenna. Figure 3(a) shows that the top view of the proposed David fractal 2×1 array antenna is two fractal geometry embedded radiating elements printed on the top side of upper substrate. The spacing between the nearest edges of the radiating

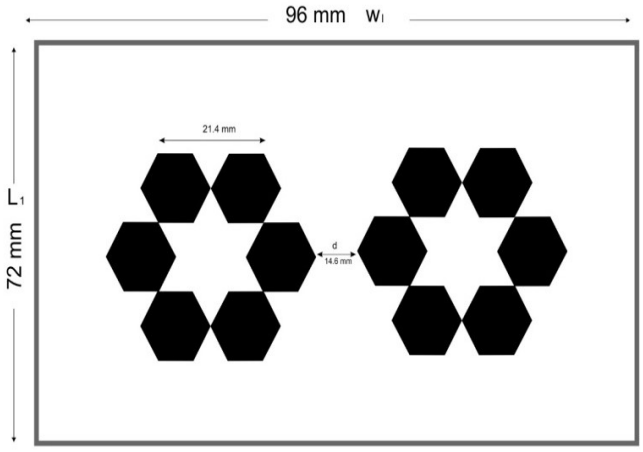

(a)

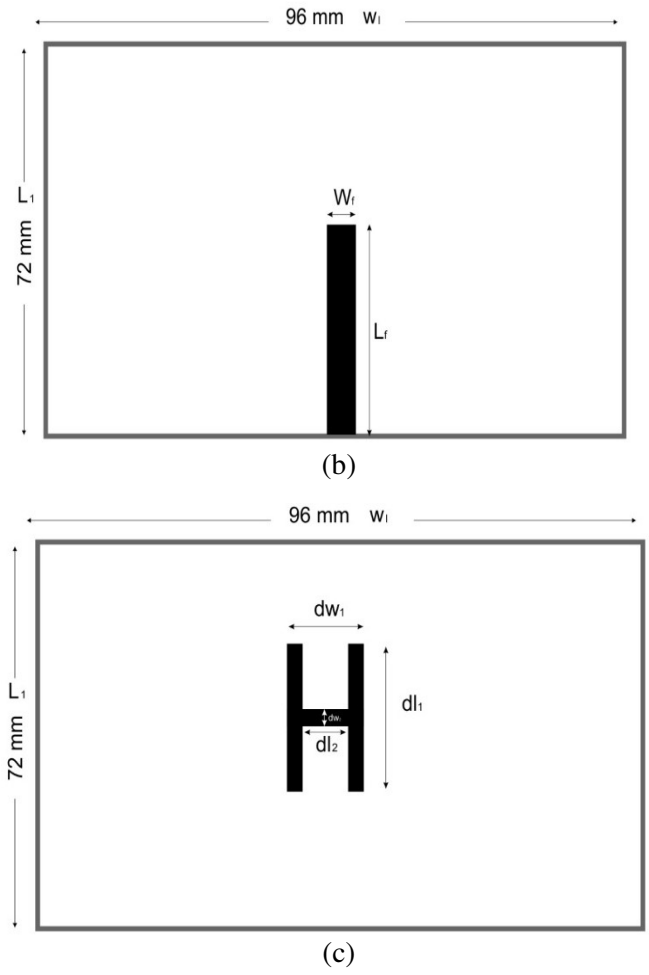

Figure 3. Geometry of the proposed triple band David fractal 2 × 1 microstrip array antenna with DGS, (a) top layer [radiating patches], (b) feed line and (c) bottom layer with defected ground structure.

elements is kept at $\lambda/12$. These two radiating elements are excited using a microstrip line as shown in Figure 3(b), which is printed on top side of the lower substrate. The back side of the lower substrate has a metallic ground plane with an H-shaped slot as shown in Figure 3(c). The optimized dimensions of the proposed antenna are given in Table 1.

Table 1. Optimised dimensions of the proposed fractal array antenna.

L_1	72 mm	W_1	96 mm	dl_2	9.6 mm
d	14.6 mm	L_f	46.4 mm	dw	2.8 mm
W_f	4.7 mm	dl_1	23.7 mm	dw_1	3.0 mm

Figure 4 illustrates the three-dimensional view of the proposed proximity fed David fractal 2 × 1 microstrip patch array antenna with defected ground structure. It consists of first iteration level David fractal geometry embedded two radiating elements etched on the top side of the upper substrate. A microstrip feed line with length L_f and width W_f is etched on the top side of the bottom substrate with ground plane on the other side of it. Side view of the proposed antenna is illustrated in Figure 5.

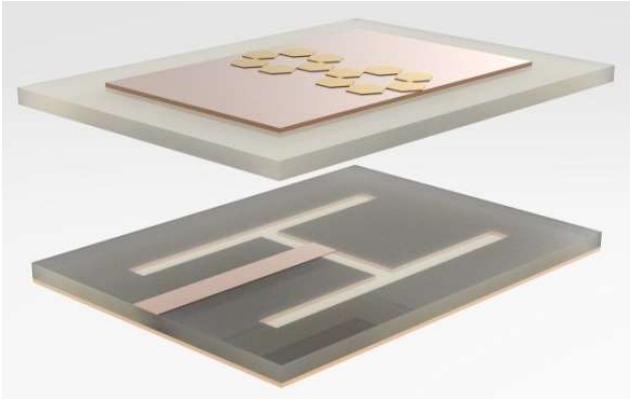

Figure 4. Three dimensional view of the proposed proximity fed David fractal 2×1 patch array antenna with DGS.

Figure 5. Side view of the proposed proximity fed David fractal 2×1 patch array antenna with DGS.

3. RESULTS AND DISCUSSION

To verify the simulated results, prototype of the simulated antenna with optimized dimensions is fabricated and tested. Figure 6 shows photographs of the fabricated proximity fed David fractal 2×1 microstrip patch array antenna with defected ground structure. The antenna is etched on an FR4 substrate having thickness of 1.6 mm, loss tangent of 0.001, and dielectric constant of 4.3. FR4 is used because it is very cheap and has excellent mechanical properties. The fabricated microstrip patch array is energized electromagnetically using a commercially available 50 Ω SMA coaxial connector.

(a) (b)

Figure 6. Photograph of the fabricated proximity fed David fractal 2×1 patch array antenna with DGS, (a) top view and (b) bottom view.

The measurements are carried out using Agilent E5063A ENA series RF network analyser, which can be used for testing passive components like antennas up to 18 GHz. The calibration of the network analyser is performed using short-open-load-through technique. After calibration, the fabricated

prototype antenna is connected to the analyser, and reflection coefficients are obtained. A broad band standard horn antenna operating between 1 GHz and 18 GHz frequencies is used for far field pattern measurements. Both the antenna under test and standard horn antenna are placed inside a fully calibrated anechoic chamber for radiation pattern measurements. The antenna under test or fabricated antenna is placed on a turn table, and the attached motor is allowed to rotate the antenna with 50 steps in both principal planes. The chambers are designed to absorb the reflections of electromagnetic radiations and to minimize interfering energy disturbances from external spurious sources.

Figure 7 illustrates the comparison between measured and simulated return loss variations with frequency. The fabricated antenna shows triple band characteristics. The three operating bands achieved in simulation are from 2.287 GHz to 2.512 GHz, with peak resonance at 2.449 GHz; 3.010 GHz to 3.37 GHz with peak resonance at 3.325 GHz and from 3.5860 GHz to 3.6490 GHz with peak resonance at 3.6160 GHz. However, measured frequency bands are 2.449 GHz to 2.752 GHz with peak resonance at 2.527 GHz; 3.280 GHz to 3.379 GHz with peak resonance at 3.329 GHz; and from 3.691 GHz to 3.793 GHz with peak resonance of 3.742 GHz. The slight discrepancy between the simulated and measured results is attributed to the changes in inductance because of fabrication imperfections and connector losses. Table 2 shows the comparison between simulated and measured return loss parameters of the proposed David fractal microstrip 2×1 patch array antenna with DGS.

In Figure 8, the comparison between simulated return loss characteristics of the proposed David fractal 2×1 array antenna with and without H shaped DGS is depicted. It is observed that the working

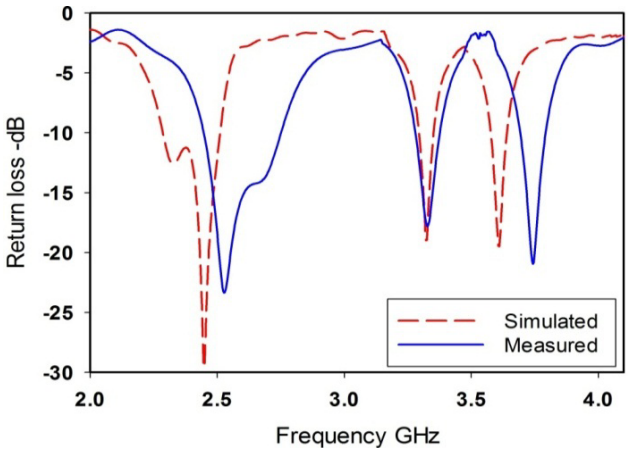

Figure 7. Simulated and measured return loss characteristics of the proximity fed David fractal 2×1 patch array antenna with DGS.

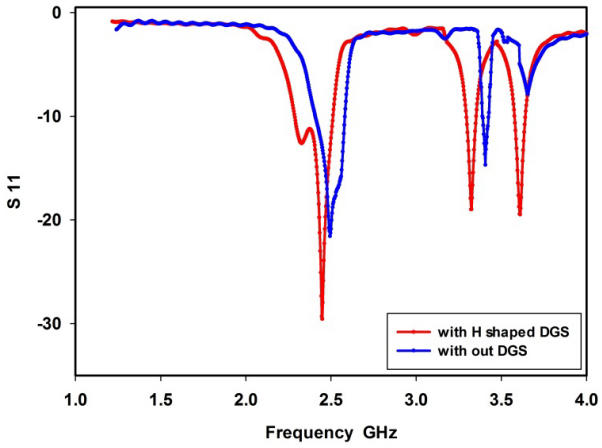

Figure 8. Comparision between simulated S_{11} characteritcis of the proposed array antenna with and without DGS.

Table 2. Comparison between simulated and measured return loss parameters of the proposed antenna.

Parameters		First Band	Second Band	Third Band
Operating frequency ranges	Simulated	2.287–2.512 GHz	3.010–3.370 GHz	3.586–3.649 GHz
	Measured	2.449–2.752 GHz	3.280–3.379 GHz	3.691–3.793 GHz
Peak resonance	Simulated	2.449 GHz	3.325 GHz	3.616 GHz
	Measured	2.527 GHz	3.329 GHz	3.742 GHz
Bandwidth	Simulated	225 MHz	69 MHz	63 MHz
	Measured	303 MHz	99 MHz	102 MHz
Fractional Bandwidth	Measured [Calculated]	11.97%	2.98%	2.74%

frequencies of the antenna with DGS are lower than that without DGS. This is because the slot etched in the ground plane changes the current distribution and extends the current path effectively. On the other hand, the S_{11} parameter increases in all three bands, which confirms the effect of DGS in enhancing antenna performance.

To provide a better understanding of the triple band behaviour of the proposed David fractal

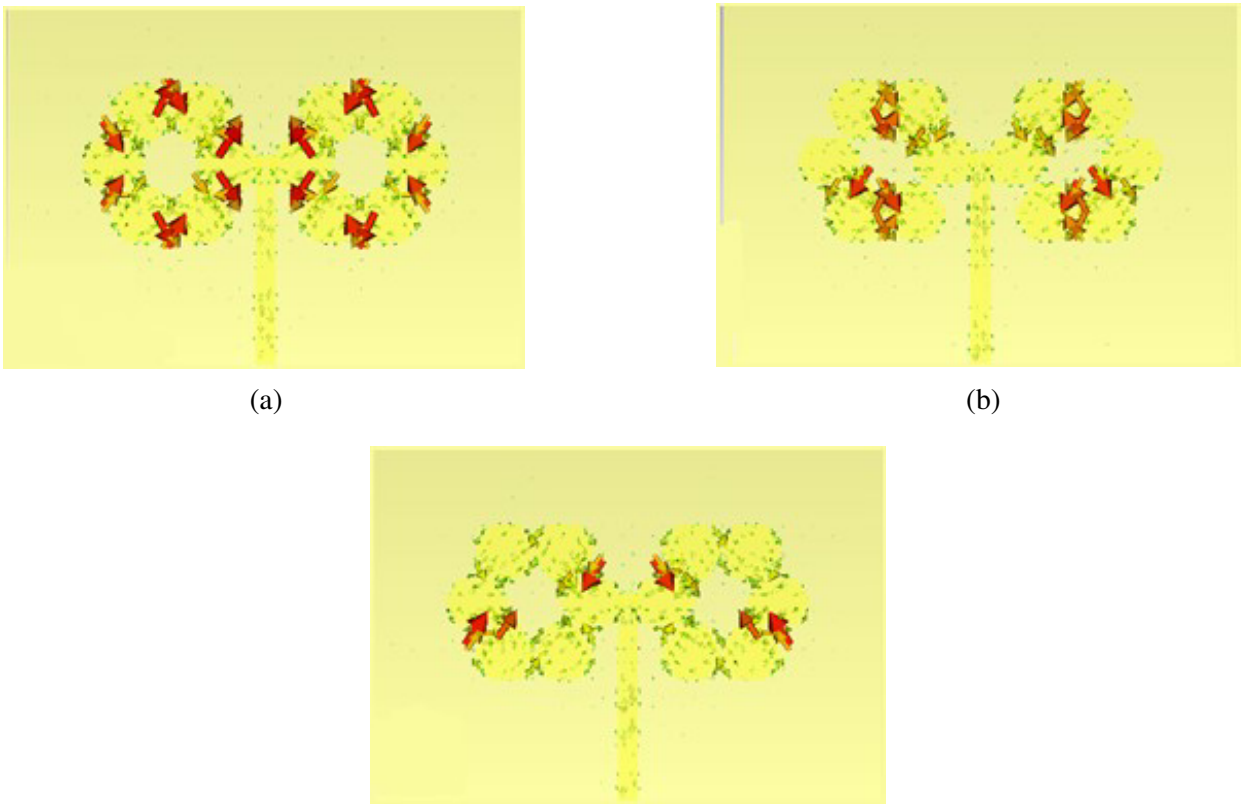

Figure 9. Simulated surface current distribution of the proposed proximity fed David fractal 2×1 microstrip patch array antenna with DGS at (a) 2.449 GHz, (b) 3.325 GHz, and (c) 3.616 GHz.

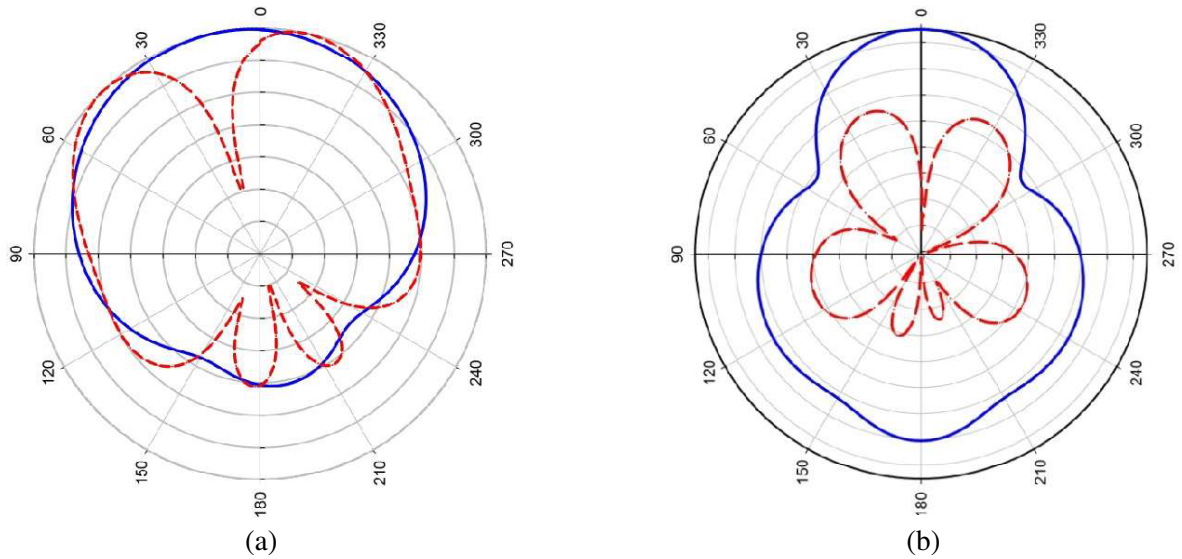

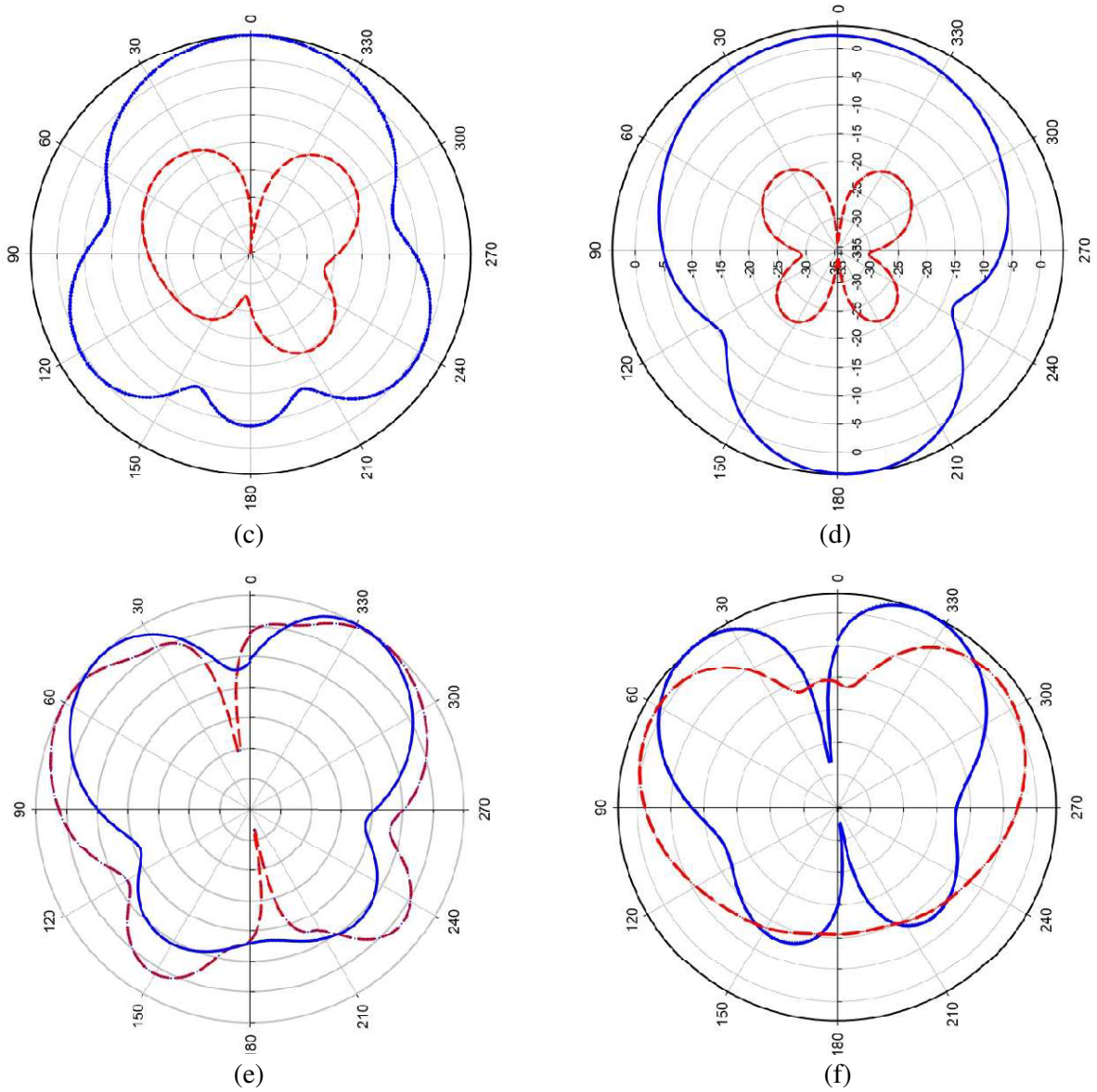

Figure 10. Measured and normalized radiation patterns of the proximity fed David fractal 2×1 array antenna with DGS at (a) & (b) lower resonant frequency of 2.527 GHz, (c) & (d) at second resonant frequency of 3.329 GHz and (e) & (f) at upper resonant frequency of 3.742 GHz [solid line represning co-poar and dotted line reprensenting cross polar]. (a) E plane, (b) H plane, (c) E plane, (d) H plane, (e) E plane, (f) H plane.

2×1 microstrip patch array antenna, surface current densities at various resonances are simulated. Figure 9 depicts the simulated surface current distributions of the proposed fractal array antenna at the resonating frequencies of 2.449 GHz, 3.325 GHz, and 3.616 GHz. In the case of lower resonant frequency as seen in Figure 9(a), strong surface current is equally distributed across both radiating patches. This surface current distribution pattern results in the formation of the radiation pattern with beam maxima towards bore sight direction. At the second resonant frequency of 3.325 GHz, it is observed that the intensity of the surface current is more concentrated on the middle areas of the radiating patches as seen in Figure 9(b). It is also observed that the current flows in the same direction, and this distribution pattern confirms the radiation pattern with beam maxima towards bore sight direction. The surface current distribution for the higher resonant frequency of 3.616 GHz is depicted in Figure 9(c). It is noted that the surface currents are not uniformly distributed across radiating elements, and the surface

currents are mainly concentrated on the edges of the radiating array elements. This current flow pattern contributes to radiation patterns with dual maxima.

The measured radiation patterns of the proposed fractal array antenna in the E plane (y-z plane) and H plane (x-z plane) are plotted at the resonant frequencies of 2.527 GHz, 3.329 GHz, and 3.742 GHz, shown in Figure 10. The electromagnetic energy distributions of the array antenna in two principal planes at the lower resonant frequency of 2.527 GHz are shown in Figure 10(a) and Figure 10(b). The radiation patterns in this frequency at both the planes are in the bore sight direction. The patterns are highly directional towards $+Z$ (positive) direction, and low cross-polarization levels are observed in both E and H planes. The HPBW of the antenna is of the order of 108° in E plane and 115° in H plane. The radiation patterns of the antenna at the second resonant frequency of 3.329 GHz are depicted in Figure 10(c) and Figure 10(d). It is observed that significant back lobes are present in the H plane. There are different proven techniques used to reduce the presence of back lobe, and a suitable method will be utilized to reduce back lobe in future work. The HPBW of the antenna is of the order of 87° in E plane and 69° in H plane. The radiation pattern of the antenna at the upper resonant frequency of 3.742 GHz is shown in Figure 10(e) and Figure 10(f). The beam maxima of the antenna radiation pattern are a few degrees away from bore sight direction on either side. This characteristic will be found useful in non-line of slight applications. The HPBW of the antenna is of the order of 91° in E plane and 59° in H plane. It is also observed that significant back lobes are present in H plane.

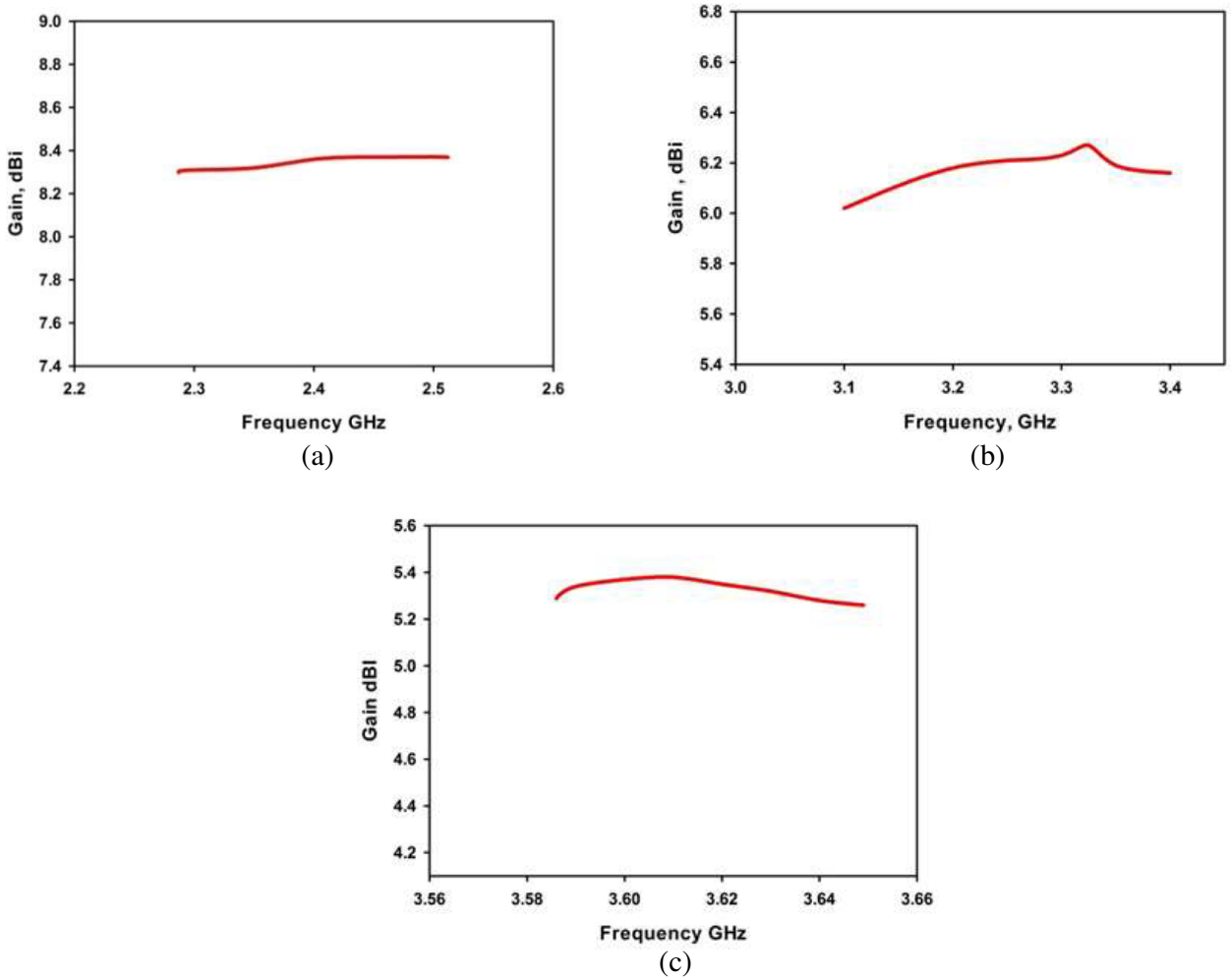

Figure 11. Measured gain with frequency of the proposed proximity fed David fractal 2×1 microstrip patch array antenna with DGS at (a) first band, (b) second band and (c) third band.

Table 3. Extracted parameters of the proposed David fractal 2×1 array antenna with DGS.

Parameters	Frequency at 2.449 GHz	Frequency at 3.325 GHz	Frequency at 3.616 GHz
	Values	Values	Values
Electric energy density	0.00184325 J/m^3	0.00179349 J/m^3	0.00172835 J/m^3
Magnetic energy density	0.0023504 J/m^3	0.0023169 J/m^3	0.0022958 J/m^3
H field peak in x direction	45.1637 A/m	43.8536 A/m	43.1638 A/m
H field peak in y direction	21.723 A/m	21.183 A/m	20.957 A/m
H field peak in z direction	78.8206 A/m	78.1739 A/m	77.6951 A/m
E field peak in x direction	5548.48 V/m	5537.28 V/m	5521.93 V/m
E field peak in y direction	9706.13 V/m	9693.37 V/m	9681.64 V/m
E field peak in z direction	9164.13 V/m	9161.37 V/m	9157.28 V/m

The measured gain of the proposed proximity coupled David fractal 2×1 microstrip patch array antenna is 8.21 dBi, 6.14 dBi, and 5.11 dBi respectively at first, second, and third resonant frequencies. Figure 11 depicts measured gain variations across the operating frequency bands. The operating bands of the antenna make it suitable for Bluetooth, Wi-Max, and Wi-Fi applications. Table 3 shows extracted parameters of the proposed triple band antenna at three different resonant frequencies.

4. CONCLUSION

This paper has proposed a triple band 2×1 microstrip patch array antenna suitable for wireless communication applications. It is designed and constructed based on the concept of a first iteration level David fractal geometry and defected ground structure. The radiating array elements are excited by electromagnetically coupling from the microstrip feedline which is printed on the top side of the bottom substrate. Compared with reference antenna, the developed array antenna has better bandwidth and operates at higher number of bands. The proposed antenna is suitable for Wi-Fi, Bluetooth, WLAN, and Wi-MAX communication standards. The antenna is printed on a low cost FR-4 substrate, and the total thickness of the antenna is at 3.2 mm. Good matching between the measured and simulated results is achieved.

REFERENCES

1. Balanis, C. A., *Antena Theory, Analysis and Design*, 3rd Edition, Wiley, New York, 2005.
2. Garg, R., P. Bhartia, I. Bahl, and A. Ittipiboon, *Microstrip Antenna Design Book*, Artech House, Boston, 2000.
3. Gong, X., L. Tong, Y. Tian, and B. Gao, "Design of a microstrip-fed hexagonal shape UWB antenna with triple notched bands," *Progress In Electromagnetics Research C*, Vol. 62, 77–87, 2016.
4. Hu, Y., Y. J. Zhang, and J. Fan, "Equivalent circuit model of coaxial probes for patch antennas," *Progress In Electromagnetics Research B*, Vol. 38, 281–296, 2012.
5. Lee, R. Q., K. F. Lee, and J. Bobinchak, "Characteristics of a two-layer electromagnetically coupled rectangular patch antennas," *Electronic Letters*, Vol. 23, No. 20, 1070–1072, Sep. 1987.
6. Mandal, T. and S. Das, "Design of a CPW fed simple hexagonal shape UWB antenna with WLAN and WiMAX band rejection characteristics," *Journal of Computational Electronics*, Vol. 14, No. 1, 300–308, Mar. 2015.
7. Kushwaha, N. and R. Kumar, "Design of slotted ground hexagonal microstrip patch antenna and gain improvement with FSS screen," *Progress In Electromagnetics Research B*, Vol. 51, 177–199, 2013.

8. Carver, K. and J. Mink, "Microstrip antenna technology," *IEEE Transactions on Antennas and Propagation*, Vol. 29, No. 1, 2–24, Jan. 1981.
9. Kshitija, T., S. Ramakrishna, S. B. Shirol, and P. Kumar, "Micro-strip patch antenna using various types of feeding techniques: An implementation," *International Conference on Intelligent Sustainable Systems (ICISS)*, 318–322, Tamil Nadu, India, Nov. 2019
10. Sahoo, A. B., N. Patnaik, A. Ravi, S. Behera, and B. B. Mangaraj, "Design of a miniaturized circular microstrip patch antenna for 5G applications," *International Conference on Emerging Trends in Information Technology and Engineering (IC-ETITE)*, 1–4, Vellore, India, May 2020.
11. Bakariya, P. S., S. Dwari, M. Sarkar, and M. K. Mandal, "Proximity-coupled multiband microstrip antenna for wireless applications," *IEEE Antennas and Wireless Propagation Letters*, Vol. 14, 646–649, Sep. 2015.
12. Casula, G. A., P. Maxia, G. Montisci, G. Valente, G. Mazzarella, and T. Pisanu, "A multiband proximity-coupled-fed flexible microstrip antenna for wireless systems," *International Journal of Antennas and Propagation*, Vol. 7, 1–7, Sep. 2016.
13. Hossain, M. B. and S. Datto, "Improvement of antenna performance using stacked microstrip patch antenna," *International Conference on Electrical, Computer and Telecommunication Engineering (ICECTE)*, 1–4, Rajshahi, Bangladesh, Feb. 2016.
14. Arya, A. K., A. Patnaik, and M. Kartikeyan, "Microstrip patch antenna with skew-F shaped DGS for dual band operation," *Progress In Electromagnetics Research M*, Vol. 19, 147–160, 2011.
15. Evangelista, T. D. S., A. G. Neto, and A. J. R. Serres, "Improved microstrip antenna with FSS superstrate for 5G NR applications," *15th European Conference on Antennas and Propagation (EuCAP)*, 1–5, Mar. 2021.
16. Nashaat, D., A. H. Elsadek, E. A. Abdallah, M. F. Iskander, and H. M. El Hennawy, "Ultrawide Bandwidth 2×2 microstrip patch array antenna using electromagnetic band-gap structure (EBG)," *IEEE Transactions on Antennas and Propagation*, Vol. 59, No. 5, May 2011.
17. Saini, J. and M. K. Garg, "PBG structured compact antenna with switching capability in lower and upper bands of 5G," *Progress In Electromagnetics Research M*, Vol. 94, 19–29, 2020.
18. Wu, B.-I., W. Wang, J. Pacheco, X. Chen, T. M. Grzegorczyk, and J. Kong, "A study of using metamaterials as antenna substrate to enhance gain," *Progress In Electromagnetics Research*, Vol. 51, 295–328, 2005.
19. Mok, W. C., S. H. Wong, K. M. Luk, and K. F. Lee, "Single-layer single-patch dual-band and triple-band patch antennas," *IEEE Transactions on Antennas and Propagation*, Vol. 61, No. 8, 4341–4344, Aug. 2013.
20. Li, P., K. M. Luk, and K. L. Lau, "A dual-feed dual-band L-probe patch antenna," *IEEE Transactions on Antennas and Propagation*, Vol. 53, No. 7, 2321–2323, Jul. 2005.
21. Joshi, M. P. and V. J. Gond, "Design and analysis of microstrip patch antenna for WLAN and vehicular communication," *Progress In Electromagnetics Research C*, Vol. 97, 163–176, 2019.
22. Mayuri, P., N. D. Rani, N. B. Subrahmanyam, and B. T. Madhav, "Design and analysis of a compact reconfigurable dual band notched UWB antenna," *Progress In Electromagnetics Research C*, Vol. 98, 141–153, 2020.
23. Abdelaziz, A., "Bandwidth enhancement of microstrip antenna," *Progress In Electromagnetic Research*, Vol. 63, 311–317, 2006.
24. Hossein, M. and J. Shahrokh, "Enhanced bandwidth of shorted patch antennas using folded-patch techniques," *IEEE Antennas and Wireless Propagation Letters*, Vol. 12, 198–201, 2013.
25. Cao, W.-Q. and W. Hong, "Bandwidth and gain enhancement for probe-fed CP microstrip antenna by loading with parasitical patches," *Progress In Electromagnetics Research Letters*, Vol. 61, 47–53, 2016.
26. Chen, Z., Y.-L. Ban, J.-H. Chen, J. L.-W. Li, and Y.-J. Wu, "Bandwidth enhancement of LTE/WWAN printed mobile phone antenna using slotted ground structure," *Progress In Electromagnetics Research*, Vol. 129, 469–483, 2012.

27. Mitra, D., D. Das, and S. R. B. Chaudhuri, "Bandwidth enhancement of microstrip line and CPW-fed asymmetrical slot antennas," *Progress In Electromagnetics Research Letters*, Vol. 32, 69–79, 2012.
28. Kim, C. S., J. S. Park, D. Aha, and J. B. Lim, "A novel I-D periodic defected ground structures for planar circuits," *IEEE Microwave and Guided Wave Letters*, Vol. 10, No. 4, 131–133, Apr. 2000.
29. Garg, R., I. Bahl, and M. Bozzi, *Micostrip Lines and Slot Lines*, 3rd Edition, Chapter 6, 287–341, Artech House, 2013.
30. Khandelwal, M. K., B. K. Kanaujia, and S. Kumar, "Defected ground structure: Fundamentals, analysis, and applications in modern wireless trends," *International Journal of Antennas and Propagation*, Vol. 2017, Article ID 2018527, 22 pages, Feb. 2017.
31. Guha, D., S. Biswas, M. Biswas, J. Y. Siddiqui, and Y. M. M. Antar, "Concentric ring-shaped defected ground structures for microstrip applications," *IEEE Antennas and Wireless Propagation Letters*, Vol. 5, No. 1, 402–405, Sept. 2006.
32. Wang, P. A., S. Gao, and W. Leng, "Miniaturized triple-band antenna with a defected ground plane for WLAN/WiMAX applications," *IEEE Antennas and Wireless Propagation Letters*, Vol. 10, 298–301, Apr. 2011.
33. Khandelwal, M. K., B. K. Kanaujia, S. Dwari, S. Kumar, and A. K. Gautam, "Triple band circularly polarized compact microstrip antenna with defected ground structure for wireless applications," *International Journal of Microwave and Wireless Technologies*, Vol. 8, No. 6, 943–953, Sept. 2016.
34. Karim, M. N. A., M. K. A. Rahim, H. A. Majid, O. Ayop, M. Abu, and F. Zubir, "Log periodic fractal koch antenna for UHF band applications," *Progress In Electromagnetics Research*, Vol. 100, 201–218, 2010.
35. Li, D. and J.-F. Mao, "Multiband multimode arched bow-shaped fractal helix antenna," *Progress In Electromagnetics Research*, Vol. 141, 47–78, 2013.
36. Waqas, M., Z. Ahmed, and M. B. Ihsan, "Multiband Sierpinski fractal antenna," *IEEE 13th International Multi-topic Conference*, Islamabad, Jul. 1–6, 2009.
37. Jibhkate, N. S. and P. L. Zade, "A compact multiband plus shape CPW fed fractal antenna for wireless application," *International Conference on Green Engineering and Technologies*, 1–5, Coimbatore, India, 2016.
38. Lopes, M., M. N. Aik, and A. Dessai, "Design and simulation of frequency reconfigurable microstrip patch antenna for C band and X band applications," *International Conference on Computing, Communication, Control and Automation*, 827–831, Pune, India, 2017.
39. Bukkawar, S. and V. Ahmed, "Square shaped fractal antenna for multiband applications," *International Conference on Smart City and Emerging Technology*, 1–4, Mumbai, 2018.
40. Kushwaha, N. and R. Kumar, "Design of slotted ground hexagonal microstrip patch antenna and gain improvement with FSS screen," *Progress In Electromagnetics Research B*, Vol. 51, 177–199, 2013.
41. Desai, A., T. K. Upadhyaya, R. Patel, S. Bhatt, and P. Mankodi, "Wideband high gain fractal antenna for wireless applications," *Progress In Electromagnetics Research Letters*, Vol. 74, 125–130, 2018.
42. Armin, B. and H. Shlomo, *Fractals in Science*, Chapter 1, Springer Verling, Berlin, 1991.
43. Abraham, J., "Investigations on multiband microstrip antennas and arrays for wireless communication applications," Ph.D. dissertation, Chapter 3, School of Technology and Applied Science, M G University, 2018.